Sensors & Actuators: B. Chemical 409 (2024) 135636

Contents lists available at ScienceDirect

Sensors and Actuators: B. Chemical

journal homepage: www.elsevier.com/locate/snb

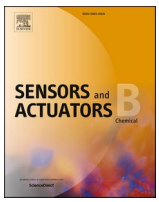

MXene-based high performance microfluidic pH sensors for electronic tongue

Hyuk Jin Kim [a], Chung Won Lee [a,b], Sohyeon Park [a], Sungkyun Choi [a], Sung Hyuk Park [a], Gi Baek Nam [a], Jung-El Ryu [a,c], Tae Hoon Eom [a], Byungsoo Kim [a], Cheol-Joo Kim [d,*], Soo Young Kim [e,*], Ho Won Jang [a,f,**]

[a] Department of Materials Science and Engineering, Research Institute of Advanced Materials, Seoul National University, Seoul 08826, Republic of Korea
[b] Department of Materials Science and Engineering, University of Central Florida, Orlando, FL 32826, United States
[c] Department of Mechanical Engineering, Massachusetts Institute of Technology, Cambridge, MA 02139, United States
[d] Department of Chemical Engineering, Pohang University of Science and Technology (POSTECH), Pohang 37673, Republic of Korea
[e] Department of Materials Science and Engineering, Korea University, Seoul 02841, Republic of Korea
[f] Advanced Institute of Convergence Technology, Seoul National University, Suwon 16229, Republic of Korea

ARTICLE INFO

Keywords:
pH sensors
2D materials
MXene
Real-time detection
Electronic tongue

ABSTRACT

The development of the electronic tongue (e-tongue) significantly relies on the monitoring of taste-inducing molecules and ions in solutions. One of the five primary flavors, sourness, has a direct correlation with pH measurement, making it essential for food assessment. However, real-time food evaluation is constrained by the high cost and limited portability of conventional taste sensors. Ti_3C_2 MXene is remarkable in the field of two-dimensional (2D) materials for its abundance of functional groups and metallic conductivity. These characteristics contribute to its enormous potential as a material for the fabrication of taste sensors with high sensitivity. This study presents the fabrication and application of reliable and reversible pH sensors based on 2D Ti_3C_2 MXene for the first time. By integrating a microfluidic channel with interdigitated electrodes (IDEs) and a Nafion layer, the sensors exhibit high selectivity for real-time detection of hydronium ions with the MXene channel. Differentiating soft drinks and evaluating the fermentation of Kimchi are demonstrated. Our work on a low-cost, high-performance MXene-based sensor will pave the way for the future of e-tongue development.

1. Introduction

In industrial processes, maintaining accurate pH levels is crucial, especially in those involving the manufacture of food and drink, pharmaceuticals, and wastewater treatment. With regard to these many applications, pH monitoring plays an essential role in assuring the production of high-quality goods, facilitating chemical reactions, and reducing the hazards of corrosion. The need of this quality assurance is becoming more apparent than ever, as the COVID-19 epidemic has increased public interest in cooking at home. Despite a direct impact of food on human health, consumers largely depend on the information provided by manufacturers. The development of e-tongue has given consumers the opportunity to obtain the nutritional information they require. E-tongues are a widely known sensing technology that contributes significantly to quality management and is designed to differentiate and analyse foods and beverages [1,2]. The analysis of sourness, one of the five flavors that e-tongue can detect, is also directly related to pH monitoring. As a result, the need for accurate pH monitoring in industries precisely matches the rise in consumer desire for reliable information about the nutritional content and potential health effects of the food. However, cost and portability problems make traditional e-tongues inappropriate for real-time monitoring of food flavor [3–5]. Moreover, ionic sensor research has encountered problems in previous decades, such as slow detection times and fluctuating base current. As a result, ionic sensors have trouble detecting in real-time, and their reliability is impacted by repeated measurements [6–8]. Therefore, a low-cost and low-power consumption e-tongue capable of real-time food monitoring is required.

* Corresponding authors.
** Corresponding author at: Department of Materials Science and Engineering, Research Institute of Advanced Materials, Seoul National University, Seoul 08826, Republic of Korea.
E-mail addresses: kimcj@postech.ac.kr (C.-J. Kim), sooyoungkim@korea.ac.kr (S.Y. Kim), hwjang@snu.ac.kr (H.W. Jang).

https://doi.org/10.1016/j.snb.2024.135636
Received 23 November 2023; Received in revised form 8 March 2024; Accepted 10 March 2024
Available online 12 March 2024

The selection of sensing materials in e-tongues is crucial to detect small changes in concentrations of ions and molecules. Diverse sensing materials, such as lipid membranes, conducting polymers, and two-dimensional (2D) materials, were utilized [3,9–13]. Among these options, 2D materials can effectively detect ions and molecules due to their unique chemical and electrical characteristics. Additionally, they have huge potential in application to real-time monitoring devices due to their superior flexible, transparent, and mechanical properties [4,10,14,15].

Previous studies of ionic sensors, including pH sensors, have shown amperometric graphs with one-side steps because a solution cannot escape the device when it is injected. In this way, the graph that increases or decreases in one direction is created because there is no process of abandoning the solution, and the base current is not constant. This means that there is a problem with the reliability and repeatability that are important to the sensor condition [6–8]. This issue can be solved by integrating a microfluidic channel with IDEs, which allows for simultaneous solution injection and withdrawal. A response current and base current will alternately be produced by the repeated injection and withdrawal of the target and washing solutions, leading to dynamic on-off functions. The target ion or molecule should be dissolved in the same solution or electrolyte as the washing solution for this purpose [4,16]. By comparing the response and base current as the solution passes through the device, the dynamic on-off functions provide the potential of real-time detection of the ionic or molecular species. Invasive technologies involve the utilization of direct contact with the sample, so facilitating the acquisition of accurate data. In contrast, non-invasive technologies employ pH measurements without direct contact, thereby conserving the integrity of the sample but potentially compromising its accuracy. The MXene pH sensor is distinguished by its invasive nature since it employs integrated microfluidic channels and electrodes to provide accurate and real-time pH measurements [7,8,17,18]. This study presents a novel pH sensor that requires the use of MXene-coated electrodes, in comparison to non-invasive techniques like optical, fluorescent, or imaging technologies. Although non-invasive techniques are effective in preserving samples, they frequently lack the real-time accuracy required for crucial industrial operations. The invasive MXene pH sensor, on the other hand, allows for precise pH measurements to be taken directly from samples. This improves operational efficiency and product quality by enabling thorough monitoring and analysis, especially in situations where continuous pH control is necessary [17,18].

MXenes, a family of 2D transition metal carbides/nitrides, are a recently discovered type of materials with abundant surface functional groups and metallic electrical conductivity. $M_{n+1}X_nT_x$ is the general formula for MXene. M stands for a transition metal (Ti, Mo, Nb, V, Zr, Ta, etc.), X is carbon or nitrogen, and n = 1, 2, or 3, and T_x is used to indicate surface functionalities. Especially, Ti_3C_2 MXene has —OH, —O, —F functional groups on its surface, which contributes to ion sensing [19–24]. These features of Ti_3C_2 MXene distinguish them apart from other candidates and provide the possibility to the development of high-performance e-tongue.

Herein, we firstly introduce pH sensor based on 2D Ti_3C_2 MXene with high response to pH variation. By coating MXenes onto IDEs through a one-step process with remarkable uniformity, we achieve enhanced selectivity and sensitivity in pH sensing, setting a new standard for sensor performance. Using the simple step of spin coating, we deposited a MXene material and a Nafion membrane. Nafion, a commonly used sieving layer, permits only small cations to migrate through while preventing the penetration of large cations. Various drinks and chemicals with different pH were utilized to demonstrate the pH sensing properties. Principal component analysis (PCA) was conducted to discriminate the drinks from the measured response data. In addition, we conducted the real-time detection during the fermentation process of Kimchi soup. Kimchi, a traditional Korean food, is prone to be fermented in room temperature. The fermentation of Kimchi occurs by microorganisms, changing the ingredients, including sugar, amino acids, vitamins and minerals. Especially, the number of lactic acid bacteria in Kimchi increases rapidly during the fermenting process. Thus, lactic acid, acetic acid, and carbonic acid gas produced by lactic acid bacteria make distinct sour flavor and smell [25–28]. We conducted an experiment to investigate the applicability of the MXene sensor by measuring the difference in acidity produced during this fermentation process. The pH value and response of the Kimchi soup were measured after fermenting Kimchi for 7 and 30 days. Therefore, our sensor enables real-time monitoring of pH changes, providing invaluable insights into dynamic processes in various industries. Through real-time measurements of pH variations in fermenting Kimchi, our sensor demonstrates remarkable selectivity and sensitivity to pH changes, emphasizing its potential in food quality control and safety applications. The results demonstrate the adaptability and efficiency of our sensor to detect pH changes in complicated food compositions, confirming it as an appropriate device for immediate monitoring in various industrial environments. Additionally, these experiments demonstrate that Nafion-coated MXene are selective and sensitive to pH change. Hence, this study is predicted to results in the development of the following generation of e-tongues.

2. Experimental section

2.1. Preparation of IDEs and microfluidic channel

The IDEs were manufactured by photolithography patterning and an e-beam evaporator depositing Pt/Ti (thickness of 100/30 nm) on SiO_2/Si substrates (thickness of SiO_2 of 300 nm). The patterned electrodes were created with a 1 mm × 1 mm size and a 5 μm gap distance. The IDE substrates were cleaned with acetone and isopropanol (IPA) using sonication for 20 min following the patterning procedure, and then they were dried by N_2 gas. In order to provide a patterned substrate for the production of the microfluidic channel, 4-inch SiO_2/Si wafer was cleaned with acetone and IPA via sonication for 20 min, and then dried with N_2 gas. The SU-8 2 was used as an adhesion layer by spin-coating on a wafer at 3000 rpm for 30 s. The soft baking process was then carried out at 65 °C for 2 min and 95 °C for 2 min. The UV light was irradiated for 2 min, followed by the soft baking process. At 180 °C for 3 min, the hard baking process was finally performed. For the photoresist (PR) layer, SU-8 50 was spin-coated at 2000 rpm for 30 s. Soft baking was conducted at 65 °C for 5 h and 95 °C for 5 h. 30 seconds of UV irradiation were followed by 3 minutes of hard baking at 180 °C. 3 min of developing, followed by a DI rinse and N_2 gas drying, were completed. The PDMS monomer and curing agent (Sylgard 184) were mixed with a weight ratio of 10:1. The prepared PDMS was poured on SU-8 template and degassed in a vacuum chamber. The patterned microfluidic channel was cut with a razor and detached after the curing process had been held for 1 h at 80 °C [4,16].

2.2. Device fabrication

Ti_3C_2 MXene was synthesized by selective etching aluminium from Ti_3AlC_2. The mixture of Ti_3AlC_2 (2 g), LiF (2 g), and 9 M HCl solution (40 mL) was maintained at 35 °C for 24 h. The etched Ti_3C_2 was washed with DI until a pH level of 6 was reached, in which the specific washing and centrifugation conditions corresponded to those from previous papers [19–21]. The surface of IDEs were treated by UV ozone for 1 h for uniform coating of Ti_3C_2 MXene. Then, Ti_3C_2 solution (5 mg mL^{-1}, 100 μL) was dropped on substrate and allowed to disperse for 30 s, followed by spin coating at 6000 rpm for 30 s. After the spin coating process, MXene samples were dried at 100 °C for 30 min. For Nafion-coated MXene, Nafion solution was spin coated on MXene. To avoid contamination, the source and drain electrodes were taped. Afterwards, Nafion 117® solution (0.1 mL) was deposited on substrate and then spin coated 6000 rpm for 30 s. The Nafion-coated MXene samples were dried at 50 °C for 30 min. By attaching the channel-patterned PDMS onto the MXene samples, the microfluidic channel MXene pH

sensor was created. The PDMS with acrylic transfer tape (Samchun chemicals) was treated with O_2 plasma for 120 s with a plasma power of 125 W and O_2 flow rate of 60 SCCM to stabilize the adhesion between the IDE and channel patterned PDMS. On the source and drain electrodes, the Cu wires were positioned and PDMS were attached [4,16].

2.3. Materials preparation and characterization

The pH solutions were prepared by mixing different ratios of DI water with KH_2PO_4 powders (Daejung, 99%) and K_2HPO_4 (Junsei, 99%) for each pH value. The pH solutions below pH 5 were prepared by mixing different ratios of DI water with Citric acid (Daejung, 99.5%) and Sodium Citrate dihydrate (Sigma Aldrich, 99%). NaCl (99.5% Daejung) and KCl (99% Daejung) powders were dissolved in DI water to prepare solutions with concentrations ranging from 1 to 5 mM. We diluted HCl (Daejung, 35.4%) solutions to yield concentrations of 1–1000 mM. MSG (monosodium glutamate, Sigma Aldrich, 99%) powder were dissolved in DI water to prepare solutions to yield concentrations of 1–1000 mM. Glucose (Sigma Aldrich, 99.5%) powder was mixed with NaOH solutions. NaOH solutions were prepared using NaOH beads (Daejung, 97%) dissolved in DI water, with a concentration 0.1 M. Quinine (Sigma Aldrich, 98%) powder was mixed with HCl solutions. We diluted HCl (Daejung, 35.4%) solutions to yield concentrations 0.1 M. The carbonated beverages were poured into a vial and sealed with parafilm. To remove the carbonic acid gas from the beverage, holes were punched in the parafilm cover and was kept in place for few days. The Nafion 117® solution was purchased from Sigma-Aldrich. Using field-emission SEM (ZEISS, MERLIN Compact), the thickness of the Nafion spin-coated samples was estimated. The topographic images of MXene were acquired from AFM (Park systems, NX-10). XPS (ThermoFisher Scientific, NEXSA) was used to analyse chemical bonding profile. Raman spectrometer (HORIBA, LabRAM HR Evolution) was used to demonstrate the existence of MXene. TEM-EDS mapping images of MXene were obtained by the TEM (JEOL, JEM-2100 F).

2.4. Measurements of ion and molecule sensing

The infusion and withdrawal of the base solution were performed using two syringe pumps (Pump 11 Elite Infusion/Withdrawal Programmable Dual Syringe, Fig. S1). The flow rate was 0.07 mL/min, and the infusion pump was paused (while the withdrawal pump continued to operate) when the target solution (100 μL) was injected using a pipette. Following the injection of the target solution, the infusion pump was turned back on for 100 s. Each solution's cycle lasted 300 s. Through the hole, a Pt wire was inserted and brought into contact with the gate source. Using an Agilent 4156 C semiconductor analyser with a source-drain voltage of 0.1 V and a gate voltage of −0.2 V, the device's electrical characteristics were assessed.

3. Results and discussion

Fig. 1a illustrates the schematic illustration of MXene pH sensor with PDMS (polydimethylsiloxane) and microfluidic channel system. Both MXene and Nafion layer were coated by facile one-step spin coating method. The sensing materials (pristine MXene and Nafion-coated MXene) were coated on IDEs, followed by a patterned PDMS deposition. The Nafion film was used to selectively penetrate small cations such as H^+, Na^+, and K^+. Fig. S1 depicts the connection of two syringe pumps to the device for liquid injection and withdrawal. Figs. 1b and 1c show the optical microscopy (OM) images of pristine MXene film and Nafion-coated MXene film, respectively. The films were highly transparent, indicating extremely low thickness. From the scanning electron microscopy (SEM) image in Fig. 1d, the pristine MXene exhibited flake shape with average size of 1 μm. In addition, the thickness of Nafion-coated MXene film was investigated by cross-sectional SEM image, as shown in Fig. 1e. Estimated from the bright region, the membrane's thickness is approximately 130 nm, and it can be predicted that large molecules or ions cannot penetrate due to their density [4,29–32]. Due to the low thickness of MXene film, atomic force microscopy (AFM) analysis was conducted, as shown in Fig. 1f. The MXene film was

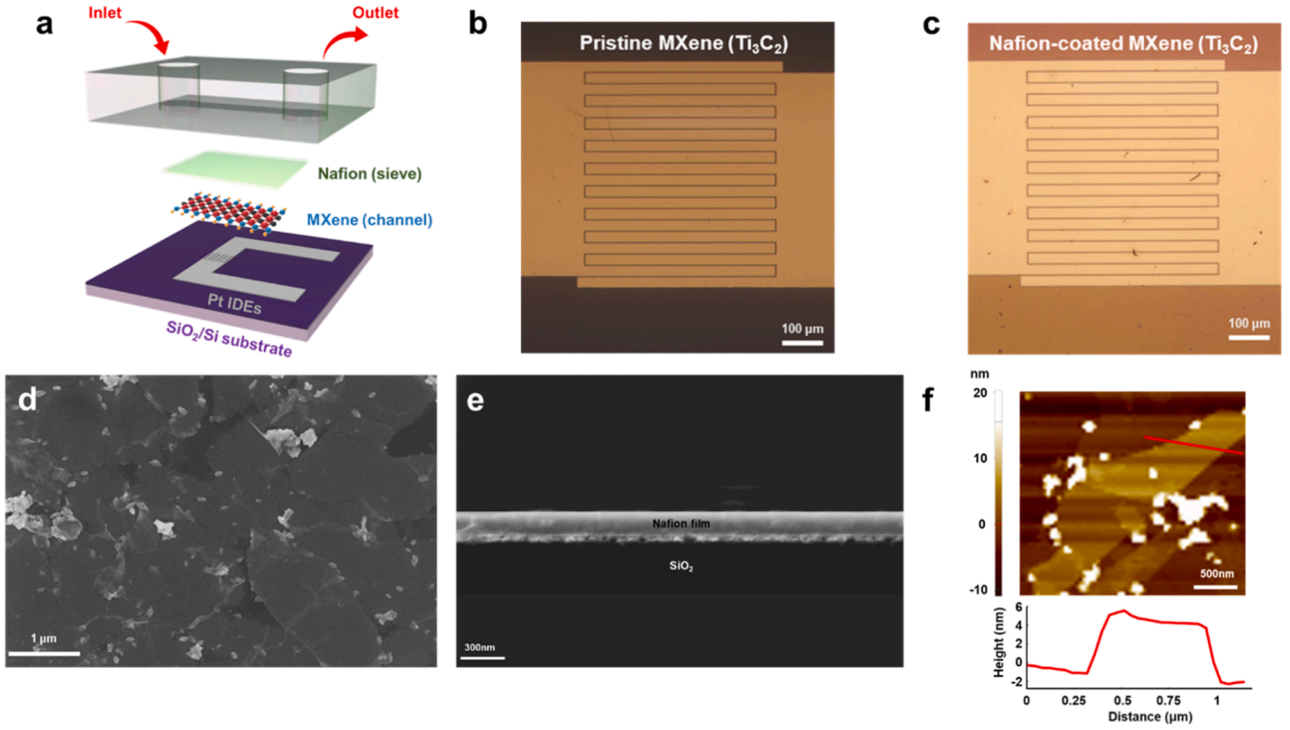

Fig. 1. Overall experiment set up and characterization of MXene film. (a) Schematic image of the microfluidic channel-integrated pH sensor. OM images of (b) pristine MXene and (c) Nafion-coated MXene. (d) SEM image of MXene film. (e) Cross-sectional SEM image of Nafion-coated MXene. (f) AFM image of MXene film and surface profile along the red line across the MXene.

consisted of stacked 2D flakes with thickness about 6 nm [33–35]. The TEM EDS mapping of Ti, O, and C in Fig. 2f confirms the distribution of the surface components. Since localized oxidation on the surface of Ti_3C_2 generates TiO_2, which modulates the Schottky barrier, this composition distribution confirms the principle of the sensing mechanism [36–38].

To investigate the functional group of Ti_3C_2 MXene in more detail, X-ray photoelectron spectroscopy (XPS) analysis was conducted. Fig. 2a shows the Ti 2p peaks for the pristine MXene, which consist of four doublets for Ti $2p_{1/2}$ and Ti $2p_{3/2}$, with each doublet separated by 5.7 eV [19,20]. The Ti $2p_{3/2}$ components at 454.7, 455.6, 457.5, and 459.2 eV correspond to Ti—C (Ti^{+}), Ti—X (Ti^{2+}), Ti_xO_y (Ti^{3+}), and TiO_2 (Ti^{4+}), respectively. C —Ti, C═C, C—O, and C—F peaks at binding energies of 281.8, 284.6, 286.1, and 289.3 eV, respectively, are depicted in Fig. 2b for the Ti_3C_2 samples. According to Fig. 2c, the O 1 s peaks are attributed to TiO_2, C—Ti—O_x, and C—Ti— $(OH)_x$ at 529.9, 530.5, and 531.9 eV, respectively. From XPS analysis, we can notice that Ti_3C_2 MXene was prepared successfully. Furthermore, the inclusion of oxygen functional groups in the Ti_3C_2 film, which serve as adsorption sites for ion/-molecule, contributes to the system's high ion/molecule sensing capability [19,36,39]. The X-ray diffraction (XRD) curves of MXene are illustrated in Fig. 2d. The diffraction peaks (002), (006), (008), and (110) observed in the Ti_3C_2 were nearly identical with the results reported for Ti_3C_2 MXene [40]. Particularly visible at $2\theta = 6.26°$ was the (002) peak, which corresponds to an inter-layer distance of 1.41 nm. Due to Ti_3C_2 oxidation, distinct peaks representing the (101), (004), and (105) planes of TiO_2 have been identified at $2\theta = 26.23°$, 37.37°, and 54.6° in the Ti_3C_2 curve [41]. The Raman spectra of pristine MXene and

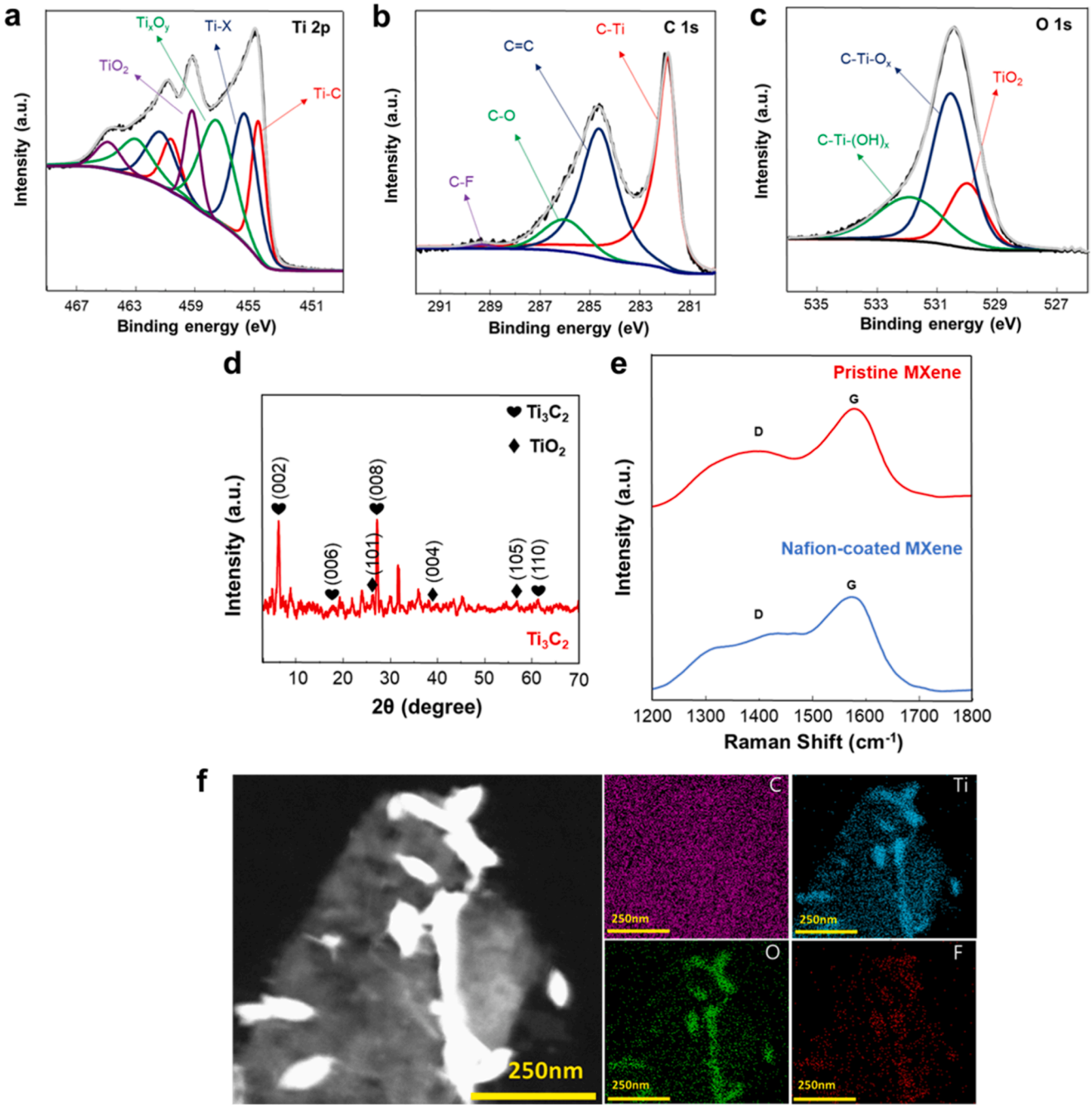

Fig. 2. Surface analysis of MXene. XPS spectra of MXene for (a) Ti 2p, (b) C 1 s, (c) O 1 s. (d) X-ray diffraction (XRD) curves of MXene. (e) Raman spectra of pristine MXene and Nafion-coated MXene. (f) TEM-EDS mapping images of MXene film.

Nafion-coated MXene were shown in Fig. 2e. The identical peak position and intensity ratio of the G and D peaks demonstrate that Nafion coating have no impact on the surface properties of MXene [42,43].

The basic sensing mechanism of pH sensor is based on ionic/molecular sensing. Especially, the pH response and selectivity highly depend on the sensing layer and sieving layer. Pristine MXene sensor and Nafion-coated MXene sensor were exposed to solution with different pH, as shown in Figs. 3a and 3b. The response of the sensing device is described by following equation (Response (%) = $(I_t\text{-}I_0)/I_0 \times 100 = \Delta I/I_0 \times 100$) where I_t and I_0 indicate the sensor's electric current in the presence of target solution and base solutions, respectively. As shown in Figs. 3a and 3b, the response of the MXene pH sensor tends to increase as

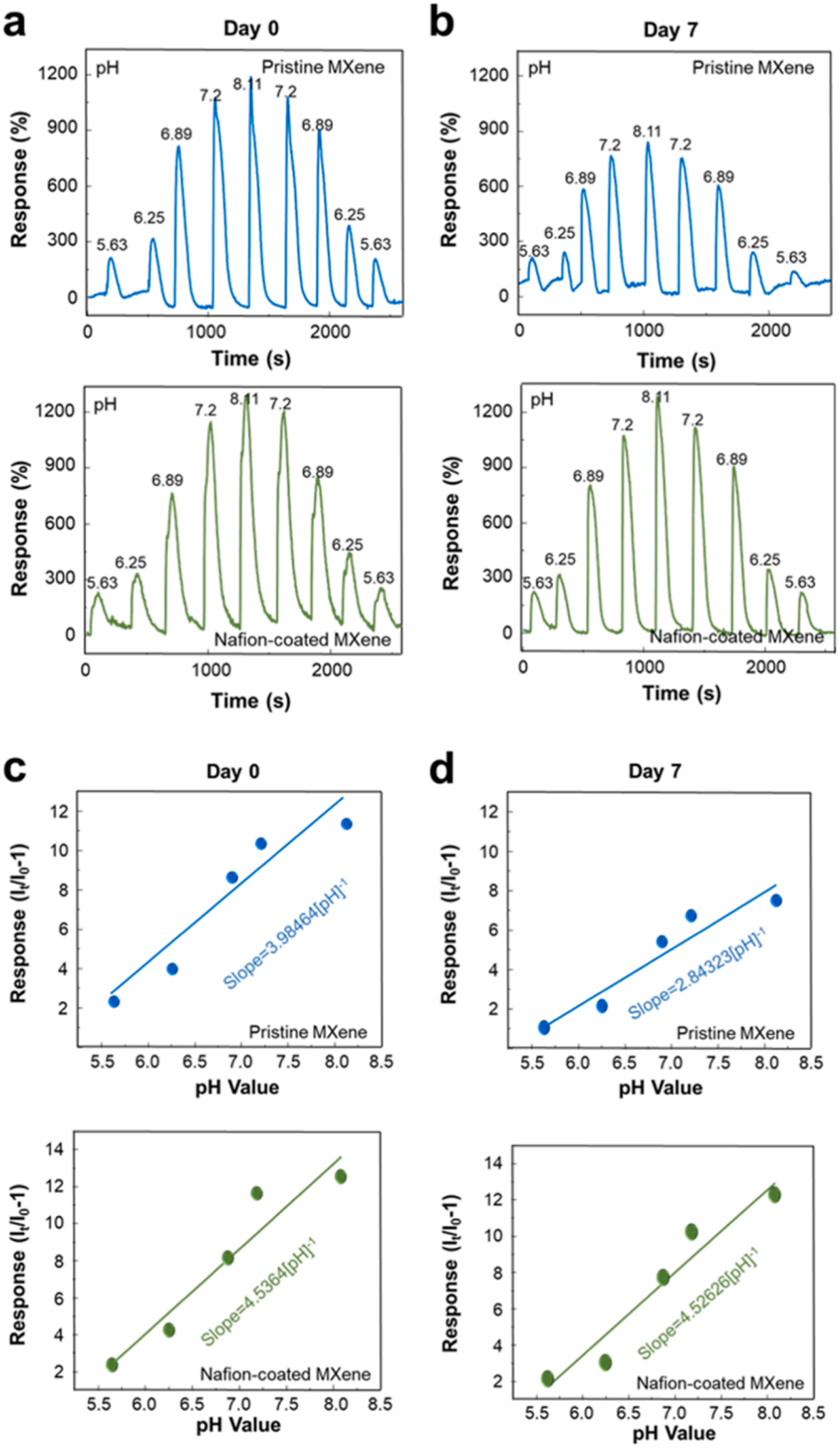

Fig. 3. pH detection characteristics of the MXene pH sensors. Response curves of pristine MXene and Nafion-coated MXene obtained (a) initially and (b) after 7 days. Linearity of sensor responses for pristine MXene and Nafion-coated MXene obtained (c) initially and (d) after 7 days.

the pH rises. However, there are stability issues for sensors designed with pristine MXene. When measured 7 days after the initial response measurement, the response and stability of pristine MXene sensor were degraded. (Figs. 3a and 3b) [4,16]. Nafion, serving as a sieving layer, can improve the response and stability to water. The Nafion film allows cations to pass through selectively, but filters other substances as a molecular sieve. The cations with larger size than the pore size of Nafion are unable to pass through the Nafion film [5,30,44]. The H_3O^+ ions can hop through the Nafion film due to the small size. The detailed hopping mechanism of H_3O^+ ions will be discussed in the later section. Moreover, the pH sensing properties were studied by exposing the sensors to solution with different pH value. The response was increased as pH was increased from 5.63 to 8.11, while the response was decreased as pH was decreased from 8.11 to 5.63. For further investigation, the response was plotted as a function of pH, as shown in Figs. 3c and 3d. The points in Figs. 3c and 3d were determined based on the average value of response to pH variation. Both pristine MXene sensor and Nafion-coated MXene sensor exhibited linear relationship between the response and pH value. The stability of pH sensor can be studied by calculating the slope between the response and pH value. For pristine MXene sensor, the slope was decreased from 3.98464 $[pH]^{-1}$ to 2.84323 $[pH]^{-1}$ after 7 days from the initial measurement. However, for Nafion-coated MXene sensor, the slope was decreased from 4.5364 $[pH]^{-1}$ to 4.52626 $[pH]^{-1}$ after 7 days from the initial measurement. Moreover, the response to five repetitive injection of solution with pH 8.11 to investigate the repeatability of pH sensors, as shown in Fig. S2. Both pristine MXene sensor and Nafion-coated MXene sensor exhibited good repeatability, where the response was consistent even after five repetitive exposure.

In addition, the response time was measured to confirm the pH sensing properties of pristine MXene sensor, and Nafion-coated MXene sensor (Fig. S3). The response time is a critical factor in evaluation of pH sensors, which is defined as the time required to achieve 90% of saturation upon exposure to target material. The response time was 14 s for pristine MXene sensor and 22 s for Nafion-coated MXene sensor, respectively. In case of pristine MXene sensor, the response time was increased to 25 s after 7 days, showing low stability. However, for Nafion-coated MXene sensor, the response time was reduced to 8 s. The reduced response time and constant response after 7 days of relaxation indicate the significant effect of Nafion on MXene-based pH sensor. Therefore, it is apparent that Nafion film not only selectively penetrates H^+ ions as a molecular sieve, but also plays a significant role in preventing performance degradation caused by the oxidation of Ti_3C_2 [4,16].

The role of Nafion on pH selectivity was investigated by measuring the response to various cations. Figs. 4a, 4b, and 4c show the response curves of Nation-coated MXene sensor to HCl, KCl, and NaCl solutions, respectively. The solutions of HCl, KCl, and NaCl were prepared with concentration ranged from 1 to 5 mM. As illustrated in Fig. 4, the response to H^+ ion was the highest among diverse cations. The response to K^+ and Na^+ exhibited little change with different ion concentration. However, the response to H^+ ion was distinguishable to different concentration of H^+ ion. This was due to the different diffusion rate of cations when penetrating the Nafion film. The previous works analysing the diffusion rate for various cations supported these results [30,31,44]. The highest cation response appeared for H^+ ion due to the smallest ion size among the substances inducing taste. This was due to ionic transfer mechanism of Nafion, as shown in Fig. 4d. Grotthuss proposed a mechanism to account for the high ionic molar conductivity of hydronium ions and the high liquid conductivity of water [45]. Based on Grotthuss mechanism, the H^+ ion can pass through Nafion. The passed H^+ ion interacts with H_2O to produce H_3O^+, allowing proton hopping to near H_2O molecule. The chain reaction of proton hopping occurs, inducing the migration of proton along the Nafion surface. The surface of Nafion contains both hydrophobic and hydrophilic regions, which is beneficial in proton hopping. The hydrophilic parts are consisted of SO^{3-}, which attract H_2O molecules. First, the produced H_3O^+ ion binds with SO^{3-}, and the proton transfers to the adjacent H_2O molecules. As a result, H_3O^+ ion is generated newly, which moves to the adjacent SO^{3-} [46–48].

It was essential to broaden the experimental approach in order to recognize the numerous details of taste perception, which expand beyond simple sourness and salty. Selectivity testing was enhanced by using solutions of glucose, quinine and MSG which means sweetness, bitterness, umami taste, in addition to the traditional NaCl and KCl

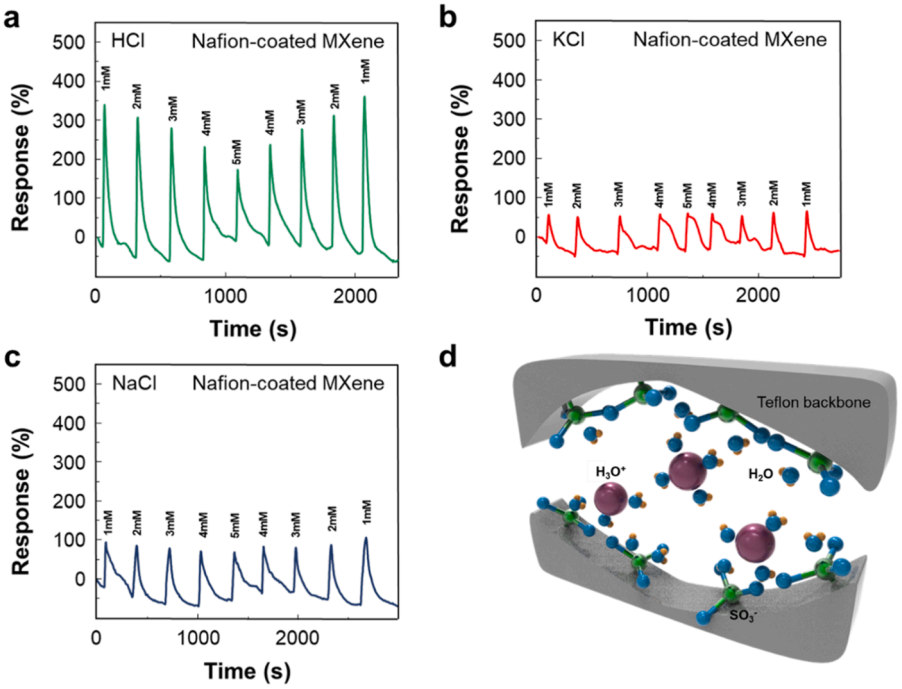

Fig. 4. Selectivity test of Nafion-coated MXene sensor. The response curves of solutions in which the cations differ in size. (a) HCl, (b) KCl, and (c) NaCl solutions were tested to concentration of 1–5 mM. (d) Ionic transfer mechanism of the Nafion sieve for selectively detecting H_3O^+.

solutions. In addition, the experiment was carried out over a significantly broader concentration range of 1–1000 mM compared to the previous range. As depicted in Fig. S4a, S4b, S4c, S4d, and S4e, it is evident that other flavor factors exhibited significantly lower sensitivity compared to hydronium ion. The result indicates the selectivity of the Nafion-coated MXene sensor. The utilization of this expanding method facilitated a specific assessment of the sensor's selectivity, yielding further understandings regarding its efficiency across diverse taste attributes.

The application of a Nafion-coated MXene sensor has been studied in both the standard pH range of 5.63–8.11 and the lower pH range below 5.0, which includes different types of food (Fig. S4f). The increased range of pH measurement highlights the effectiveness of the sensor in detecting a wider range of acidity levels. Therefore, our research confirms the sensor's strong performance, expanding its usefulness outside the typical pH range and demonstrating its adaptability in various acidic conditions. The pH sensing measurements were conducted with various real beverages, including Coke, orange juice, Sprite, and Gatorade. The beverages were injected to pH sensors with five pulses, as shown in Fig. S5 (pristine MXene) and Fig. S6 (Nafion-coated MXene). The response of both pristine MXene sensor and Nafion-coated MXene sensor to beverages was plotted, as shown in Figs. 5a and 5b. For pristine MXene sensor, the response to beverages showed little difference, indicating poor selectivity. In the case of Nafion-coated MXene sensor, the response to Gatorade was much higher than other beverages with high selectivity. The relationship between sensor outputs and pH values was established by fitting the pH values of each beverage to their corresponding sensor responses, as depicted in Fig. S7. The figure clearly demonstrates a noticeable trend where the sensor response rises as the pH levels increase, exactly like the behavior found in pH solution testing. The consistency found in this study not only confirms the sensor's ability to accurately detect pH in standard solutions, but also verifies its proficiency in pH detection across different types of beverages, including regularly encountered soft drinks. To further study the beverage selectivity, PCA was conducted for pristine MXene sensor and Nafion-coated MXene sensor, as shown in Figs. 5c and 5d. For the analysis, the response, response time, and base current values were collected from Fig. S5 and S6. Then, the collected values with different scale and unit were changed into normalized values. The two principal components with the highest importance were selected as the x- and y-axis for 2D plots to prove effective selectivity [4,16]. In addition, as shown in Fig. 5c, the PCA data of pristine MXene sensor reveals that data points are highly distributed, implying that pristine MXene sensor has low selectivity to beverages. In the case of Nafion-coated MXene sensor, the data points for each beverage were placed nearby with high selectivity. The PCA results indicate that pristine MXene is not appropriate for distinguishing real beverages due to the less difference in sensing parameters. In contrast, the Nafion coating enabled the efficient discrimination of real beverages, which is promising in e-tongue technologies.

The practicality of Nafion-coated MXene sensor was further studied using Kimchi, a traditional Korean food. Kimchi easily ripens at ambient atmosphere and generates various acids, resulting in sour flavor. Figs. 6a, 6b, and 6c show the response curves of Nafion-coated MXene sensor to Kimchi. The response was measured at the starting day, after 7 days, and after 30 days for fermentation. As fermentation proceeds, the acidity increases; consequently, the pH value decreases. This can be confirmed by the response measurement, where the response was decreased after 7 days and 30 days of fermentation. The decreased pH during fermentation resulted in decreased response. The images of fermentation of Kimchi were shown in Figs. 6d and 6e. Due to the generation of various acids, the distinct color variation was investigated. Fig. 6f depicts a comparison of the pH change and response change of a Nafion-coated MXene sensor to Kimchi soup over time. Overall, this demonstrates that the pH and response values decrease as the acidity of Kimchi increases over time. Therefore, based on the collected data, it can be confirmed that the Nafion-coated MXene device can detect liquids that can be easily observed in real time.

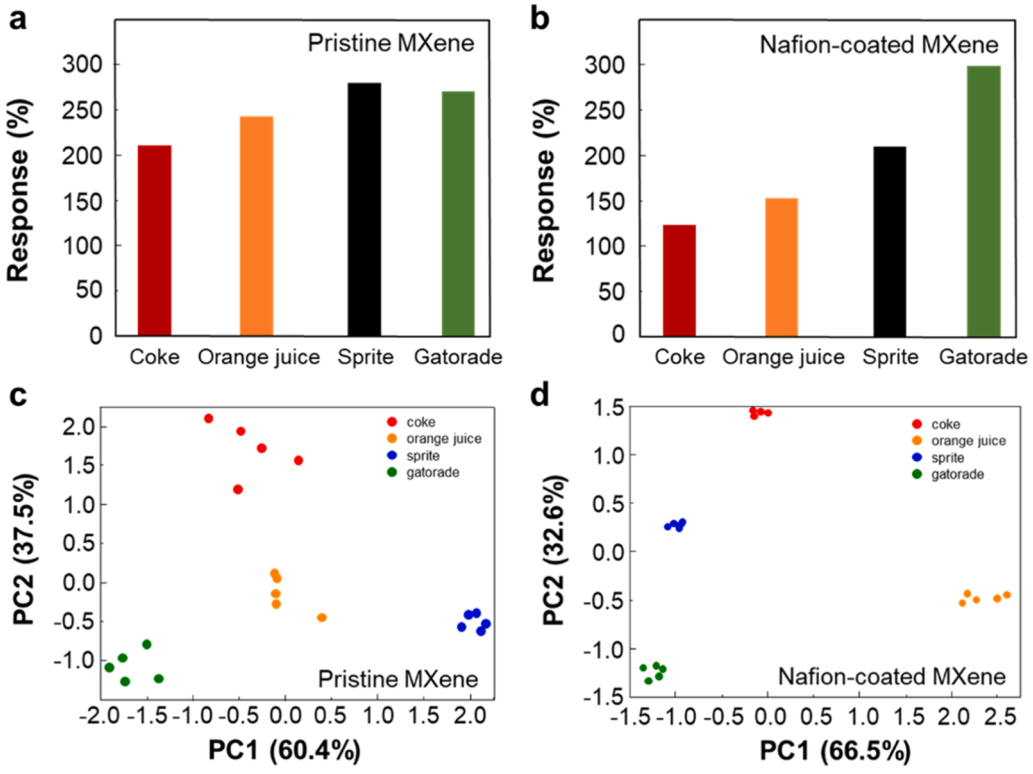

Fig. 5. Responses and PCA plots to real beverages. Response comparison of (a) pristine MXene sensor, (b) Nafion-coated MXene sensor to four soft drinks (Coke, orange juice, Sprite, and Gatorade). PCA plots of (c) pristine MXene sensor and (d) Nafion-coated MXene sensor for actual beverages.

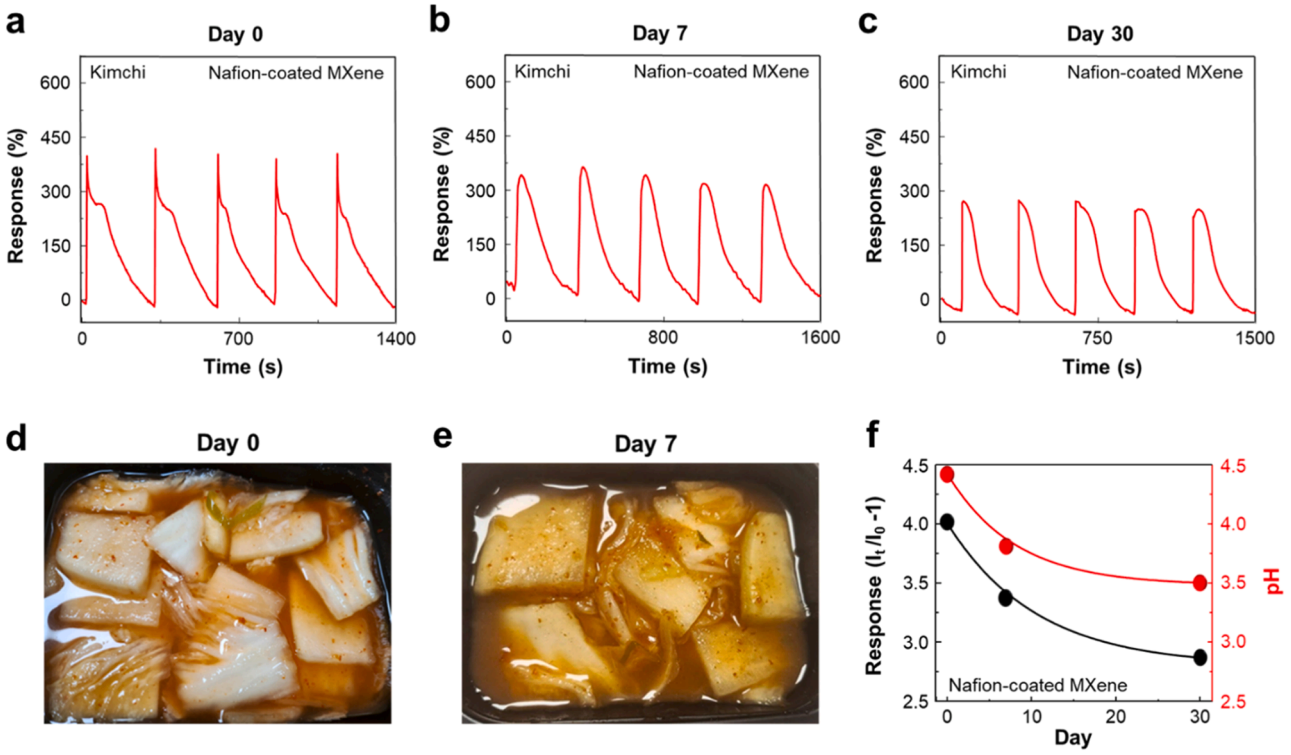

Fig. 6. Response plots and real images of Kimchi. Repetitive test for Kimchi soup after (a) 0, (b) 7, and (c) 30 days. Real images of Kimchi soup collected (d) before and (e) after one week of fermentation. (f) Comparing the response change and pH change of a Nafion-coated MXene sensor to Kimchi soup over time is illustrated in the graph.

The outstanding pH sensing properties of Nafion-coated MXene can be explained by Schottky barrier modulation between TiO_2 and Ti_3C_2 MXene. As shown in Fig. 2d, the surface of Ti_3C_2 MXene contains oxidized region, where TiO_2 is generated. Thus, the Schottky barrier is formed between TiO_2 and Ti_3C_2 MXene. Ions with various types of charges (H_3O^+/OH^- ion), are attracted to Ti_3C_2 surface and then released. This causes a change in the barrier, which is the primary mechanism of pH sensing. Fig. 7a depicts the mechanism of liquid sensors based on the formation of Schottky barriers in hybrid TiO_2/Ti_3C_2 structure. We constructed a band diagram of the TiO_2/Ti_3C_2 interface to demonstrate the formation of Schottky barrier between the metallic Ti_3C_2 and semiconducting TiO_2. The adsorbed H_3O^+ ion can increase the

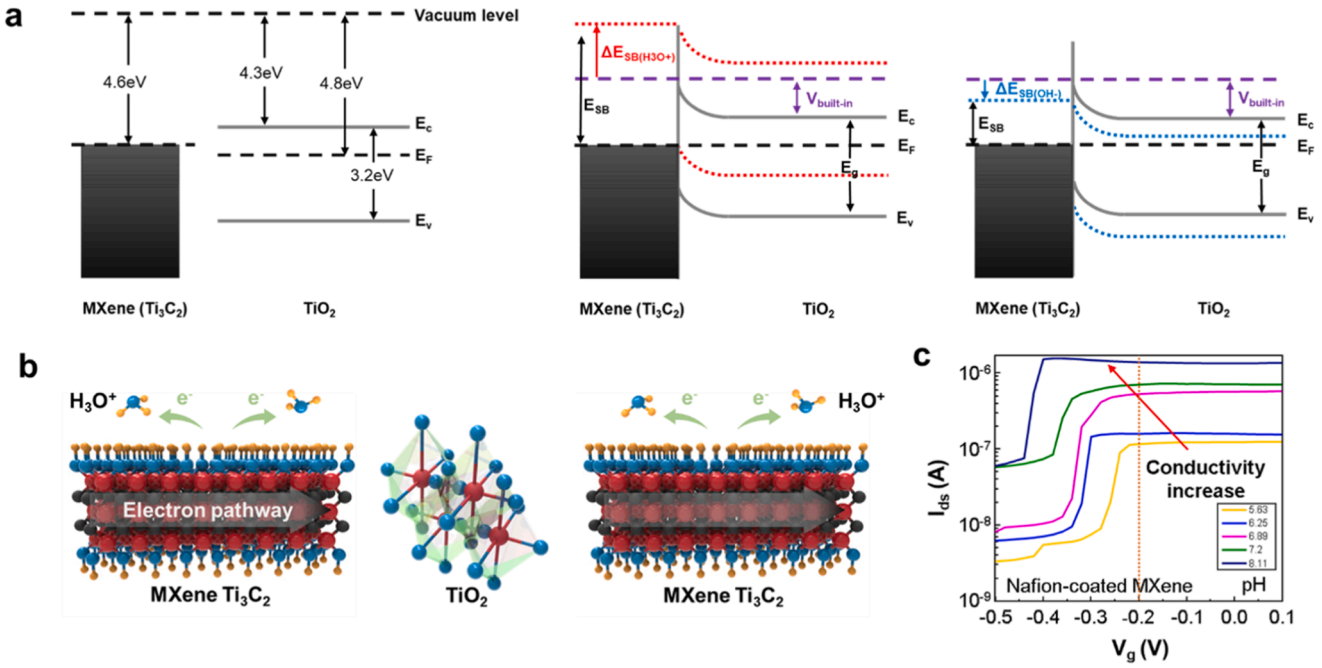

Fig. 7. Schematic illustration of the sensing mechanism of MXene pH sensor. (a) Schottky barrier modulation upon exposure to H_3O^+ and OH^- ions. (b) Ion sensing mechanism of MXene pH sensor. (c) Transfer characteristic of Nafion-coated MXene sensor.

electron potential barrier, thereby restricting the electron pathway. H_3O^+ ion functions as an electron acceptor and raises the resistance of both Ti_3C_2 and TiO_2/Ti_3C_2. The OH^- ion likewise modifies the electron potential barrier in the case of the OH^- ion, resulting reduction of potential barrier to facilitate the passage of the electrons. Fig. 7b provides a schematic illustration of ion sensing mechanism where H_3O^+ ion is adsorbed on Ti_3C_2 and TiO_2/Ti_3C_2. This Schottky barrier modulation influences the electron path, allowing for efficient ion sensing [19].

Fig. 7c depicts the evaluation of the transfer characteristics of Nafion-coated MXene sensor in different pH value. The I_{ds} (drain-source current) was measured as a function of V_g (gate voltage) to pH variation. Because the electron potential barrier rises when H_3O^+ is adsorbed, it obstructs the electron route. The response rises with pH due to the lowered electron potential barrier when OH^- is adsorbed, which facilitates the electron transport.

4. Conclusion

In summary, we have successfully demonstrated a MXene pH sensor that detects H^+ ions selectively and can be fabricated using a simple process. The microfluidic channel allows the injection and ejection of solutions, which maintain base current and enable real-time detection with IDE substrate integration. In contrast to previous research on ionic sensors, this sensor structure is beneficial in enhancing sensing properties, including high reliability and a rapid detection time. Ti_3C_2 MXene was coated with a Nafion film to improve selectivity and repeatability. Moreover, the Nafion film prevents large molecules and ions from passing through while allowing small ions such as H^+ to pass through, resulting in selective detection. Actual beverages such as Coke, orange juice, Sprite, and Gatorade were used in the experiment for practical testing of the device. Through PCA, each drink was distinguished from the others, and the selectivity of the device was demonstrated. In addition, the practicability of device was evaluated by measuring the pH change and response according to the maturation time of Kimchi, a traditional Korean food. Likewise, the simple fabrication method provided a novel viewpoint for current ionic and molecular sensors. The MXene-based pH sensor integrated with microfluidic channels can detect actual liquids and H^+ ions in real time and pave the way to the development of an electronic tongue.

CRediT authorship contribution statement

Cheol-Joo Kim: Conceptualization. **Soo Young Kim:** Conceptualization. **Ho Won Jang:** Writing – review & editing, Supervision, Conceptualization. **Hyuk Jin Kim:** Writing – original draft, Visualization, Validation, Investigation, Conceptualization. **Chung Won Lee:** Conceptualization. **Jung-El Ryu:** Data curation. **Tae Hoon Eom:** Writing – review & editing. **Byungsoo Kim:** Writing – review & editing. **Sohyeon Park:** Data curation. **Sungkyun Choi:** Data curation. **Sung Hyuk Park:** Data curation. **Gi Baek Nam:** Data curation.

Declaration of Competing Interest

The authors declare that they have no known competing financial interests or personal relationships that could have appeared to influence the work reported in this paper.

Data availability

Data will be made available on request.

Acknowledgements

This work was financially supported by Nano Material Technology Development Program (2022M3H4A1A01011993) through NRF (National Research Foundation of Korea), funded by the Ministry of Science and ICT. This work was also financially supported by "Cooperative Research Program for Agriculture Science and Technology Development (Project No. PJ01706703)" Rural Development Administration, Republic of Korea. This research was also supported by Research Institute of Advanced Materials (RIAM), Inter University Semiconductor Research Center (ISRC), and Institute of Engineering Research at Seoul National University.

Appendix A. Supporting information

Supplementary data associated with this article can be found in the online version at doi:10.1016/j.snb.2024.135636.

References

[1] Y. Tahara, K. Toko, Electronic tongues-a review, IEEE Sens. J. 13 (2013) 3001–3011.
[2] M. Podrazka, E. Báczyńska, M. Kundys, P.S. Jeleń, E.W. Nery, Electronic tongue-A tool for all tastes? Biosensors 8 (2017) 1–24.
[3] A. Riul, C.A.R. Dantas, C.M. Miyazaki, O.N. Oliveira, Recent advances in electronic tongues, Analyst 135 (2010) 2481–2495.
[4] C.W. Lee, J.M. Suh, S. Choi, S.E. Jun, T.H. Lee, J.W. Yang, S.A. Lee, B.R. Lee, D. Yoo, S.Y. Kim, D.S. Kim, H.W. Jang, Surface-tailored graphene channels, Npj 2D Mater. Appl. 5 (2021) 1–13.
[5] Y. Qin, A.U. Alam, S. Pan, M.M.R. Howlader, R. Ghosh, N.X. Hu, H. Jin, S. Dong, C. H. Chen, M.J. Deen, Integrated water quality monitoring system with pH, free chlorine, and temperature sensors, Sens. Actuators B Chem. 255 (2018) 781–790.
[6] Ohno, K. Maehashi, Y. Yamashiro, K. Matsumoto, Electrolyte-gated graphene field-effect transistors for detecting ph and protein adsorption, Nano Lett. 9 (2009) 3318–3322.
[7] Y. Tang, L. Zhen, J. Liu, J. Wu, Rapid antibiotic susceptibility testing in a microfluidic pH sensor, Anal. Chem. 85 (2013) 2787–2794.
[8] S.K. Ameri, P.K. Singh, S.R. Sonkusale, Three dimensional graphene transistor for ultra-sensitive pH sensing directly in biological media, Anal. Chim. Acta 934 (2016) 212–217.
[9] M. Habara, H. Ikezaki, K. Toko, Study of sweet taste evaluation using taste sensor with lipid/polymer membranes, Biosens. Bioelectron. 19 (2004) 1559–1563.
[10] C.W. Lee, T.H. Eom, S.H. Cho, H.W. Jang, Chemical sensors based on graphene and 2D graphene analogs, Adv. Sens. Res 2 (2023) 2200057.
[11] V. Parra, Á.A. Arrieta, J.A. Fernández-Escudero, H. García, C. Apetrei, M. L. Rodríguez-Méndez, J.A. d Saja, E-tongue based on a hybrid array of voltammetric sensors based on phthalocyanines, perylene derivatives and conducting polymers: Discrimination capability towards red wines elaborated with different varieties of grapes, Sens. Actuators, B Chem. 115 (2006) 54–61.
[12] C.E. Borato, F.L. Leite, O.N. Oliveira, L.H.C. Mattoso, Efficient taste sensors made of bare metal electrodes, Sens. Lett. 4 (2006) 155–159.
[13] E.S. Medeiros, R. Gregório, R.A. Martinez, L.H.C. Mattoso, A taste sensor array based on polyaniline nanofibers for orange juice quality assessment, Sens. Lett. 7 (2009) 24–30.
[14] F. Ye, B. Xu, R. Chen, R. Li, G. Chang, The influence of nano- and micron-size of mxene flakes on the electrochemical performance, Electron. Mater. Lett. 19 (2023) 527–533.
[15] L. Le Qiao, F.J. Zhang, C.M. Kai, C. Liu, Y.R. Wang, W.C. Oh, Preparation of 2D/2D g-C_3N_4/Ti_3C_2 MXene composites by calcination synthesis method for visible light photocatalytic degradation of tetracycline, J. Korean Ceram. Soc. 60 (2022) 790–797.
[16] C.W. Lee, S.E. Jun, S.J. Kim, T.H. Lee, S.A. Lee, J.W. Yang, J.H. Cho, S. Choi, C. joo Kim, S.Y. Kim, H.W. Jang, Rationally designed graphene channels for real-time sodium ion detection for electronic tongue, InfoMat 5 (2023) 1–16.
[17] F. Wang, Y. Raval, H. Chen, T. Tzeng, J. Desjardins, J. Anker, Development of luminescent pH sensor films for monitoring bacterial growth through tissue, Adv. Healthc. Mater. 3 (2014) 221–229.
[18] X. Zhu, Q. Lin, P. Chen, A novel pH sensor which could respond to multi-scale pH changes: Via different fluorescence emissions, N. J. Chem. 40 (2016) 4562–4565.
[19] J. Choi, Y.J. Kim, S.Y. Cho, K. Park, H. Kang, S.J. Kim, H.T. Jung, In situ formation of multiple schottky barriers in a Ti_3C_2 MXene film and its application in highly sensitive gas sensors, Adv. Funct. Mater. 30 (2020) 2003998.
[20] S.J. Kim, H.J. Koh, C.E. Ren, O. Kwon, K. Maleski, S.Y. Cho, B. Anasori, C.K. Kim, Y. K. Choi, J. Kim, Y. Gogotsi, H.T. Jung, Metallic $Ti_3C_2T_x$ MXene gas sensors with ultrahigh signal-to-noise ratio, ACS Nano 12 (2018) 986–993.
[21] M. Alhabeb, K. Maleski, B. Anasori, P. Lelyukh, L. Clark, S. Sin, Y. Gogotsi, Guidelines for synthesis and processing of two-dimensional titanium carbide ($Ti_3C_2T_x$ MXene), Chem. Mater. 29 (2017) 7633–7644.
[22] M. Naguib, O. Mashtalir, J. Carle, V. Presser, J. Lu, L. Hultman, Y. Gogotsi, M. W. Barsoum, Two-dimensional transition metal carbides, ACS Nano 6 (2012) 1322–1331.
[23] Y.Z. Zhang, K.H. Lee, D.H. Anjum, R. Sougrat, Q. Jiang, H. Kim, H.N. Alshareef, MXenes stretch hydrogel sensor performance to new limits, Sci. Adv. 4 (2018) 1–7.
[24] A. Lipatov, H. Lu, M. Alhabeb, B. Anasori, A. Gruverman, Y. Gogotsi, A. Sinitskii, Elastic properties of 2D $Ti_3C_2T_x$ MXene monolayers and bilayers, Sci. Adv. 4 (2018) 1–7.

[25] J.K. Patra, G. Das, S. Paramithiotis, H.S. Shin, Kimchi and other widely consumed traditional fermented foods of Korea: a review, Front. Microbiol. 7 (2016) 1493.
[26] J.Y. Jung, S.H. Lee, C.O. Jeon, Kimchi microflora: History, current status, and perspectives for industrial kimchi production, Appl. Microbiol. Biotechnol. 98 (2014) 2385–2393.
[27] K.Y. Park, J.K. Jeong, Y.E. Lee, J.W. Daily, Health benefits of kimchi (Korean fermented vegetables) as a probiotic food, J. Med. Food 17 (2014) 6–20.
[28] J.J. Lee, Y.J. Choi, M.J. Lee, S.J. Park, S.J. Oh, Y.R. Yun, S.G. Min, H.Y. Seo, S. H. Park, M.A. Lee, Effects of combining two lactic acid bacteria as a starter culture on model kimchi fermentation, Food Res. Int. 136 (2020) 109591.
[29] R.R. Passos, V.A. Paganin, E.A. Ticianelli, Studies of the performance of PEM fuel cell cathodes with the catalyst layer directly applied on Nafion membranes, Electrochim. Acta 51 (2006) 5239–5245.
[30] I.A. Stenina, P. Sistat, A.I. Rebrov, G. Pourcelly, A.B. Yaroslavtsev, Ion mobility in Nafion-117 membranes, Desalination 170 (2004) 49–57.
[31] A. Lehmani, P. Turq, M. Périé, J. Périé, J.P. Simonin, Ion transport in Nafion® 117 membrane, J. Electroanal. Chem. 428 (1997) 81–89.
[32] A.H. Avci, D.A. Messana, S. Santoro, R.A. Tufa, E. Curcio, G. Di Profio, E. Fontananova, Energy harvesting from brines by reverse electrodialysis using nafion membranes, Membr. (Basel) 10 (2020) 1–16.
[33] X. Xu, T. Guo, M.K. Hota, H. Kim, D. Zheng, C. Liu, M.N. Hedhili, R.S. Alsaadi, X. Zhang, H.N. Alshareef, High-Yield $Ti_3C_2T_x$ MXene–MoS_2 integrated circuits, Adv. Mater. 34 (2022) 2107370.
[34] X. Sheng, S. Li, H. Huang, Y. Zhao, Y. Chen, L. Zhang, D. Xie, Anticorrosive and UV-blocking waterborne polyurethane composite coating containing novel two-dimensional Ti_3C_2 MXene nanosheets, J. Mater. Sci. 56 (2021) 4212–4224.
[35] S. Ahn, T.H. Han, K. Maleski, J. Song, Y.H. Kim, M.H. Park, H. Zhou, S. Yoo, Y. Gogotsi, T.W. Lee, A 2D titanium carbide mxene flexible electrode for high-efficiency light-emitting diodes, Adv. Mater. 32 (2020) 2000919.
[36] C. Peng, X. Yang, Y. Li, H. Yu, H. Wang, F. Peng, Hybrids of two-dimensional Ti_3C_2 and TiO_2 Exposing {001} Facets toward Enhanced Photocatalytic Activity, ACS Appl. Mater. Interfaces 8 (2016) 6051–6060.
[37] J. Low, L. Zhang, T. Tong, B. Shen, J. Yu, TiO_2/MXene Ti_3C_2 composite with excellent photocatalytic CO_2 reduction activity, J. Catal. 361 (2018) 255–266.
[38] D.Y. Zhang, H. Liu, M.R. Younis, S. Lei, Y. Chen, P. Huang, J. Lin, In-situ TiO_{2-x} decoration of titanium carbide MXene for photo/sono-responsive antitumor theranostics, J. Nanobiotechnology. 20 (2022) 1–14.
[39] T.S. Mathis, K. Maleski, A. Goad, A. Sarycheva, M. Anayee, A.C. Foucher, K. Hantanasirisakul, C.E. Shuck, E.A. Stach, Y. Gogotsi, Modified MAX phase synthesis for environmentally stable and highly conductive Ti_3C_2 MXene, ACS Nano 15 (2021) 6420–6429.
[40] M. Naguib, M. Kurtoglu, V. Presser, J. Lu, J. Niu, M. Heon, L. Hultman, Y. Gogotsi, M.W. Barsoum, Two-dimensional nanocrystals produced by exfoliation of Ti_3AlC_2, Adv. Mater. 23 (2011) 4248–4253.
[41] N. Liu, L. Yu, B. Liu, F. Yu, L. Li, Y. Xiao, J. Yang, J. Ma, Ti_3C_2-MXene partially derived hierarchical 1D/2D TiO_2/Ti_3C_2 heterostructure electrode for high-performance capacitive deionization, Adv. Sci. 10 (2023) 2204041.
[42] X. Li, X. Yin, M. Han, C. Song, H. Xu, Z. Hou, L. Zhang, L. Cheng, Ti_3C_2 MXenes modified with: In situ grown carbon nanotubes for enhanced electromagnetic wave absorption properties, J. Mater. Chem. C 5 (2017) 4068–4074.
[43] W. Lv, J. Zhu, F. Wang, Y. Fang, Facile synthesis and electrochemical performance of TiO_2 nanowires/Ti_3C_2 composite, J. Mater. Sci. Mater. Electron. 29 (2018) 4881–4887.
[44] G. Xie, T. Okada, Water transport behavior in nafion 117 Membranes, J. Electrochem. Soc. 142 (1995) 3057–3062.
[45] K.R. Maiyelvaganan, S. Kamalakannan, S. Shanmugan, M. Prakash, F.X. Coudert, M. Hochlaf, Identification of a Grotthuss proton hopping mechanism at protonated polyhedral oligomeric silsesquioxane (POSS) – water interface, J. Colloid Interface Sci. 605 (2022) 701–709.
[46] N. Agmon, The Grotthuss mechanism, Chem. Phys. Lett. 244 (1995) 456–462.
[47] P. Choi, N.H. Jalani, R. Datta, Thermodynamics and proton transport in Nafion II. Proton diffusion mechanisms and conductivity, J. Electrochem. Soc. 152 (2005) E123–E130.
[48] S. Bukola, Y. Liang, C. Korzeniewski, J. Harris, S. Creager, Selective proton/deuteron transport through nafion|graphene|nafion sandwich structures at high current density, J. Am. Chem. Soc. 140 (2018) 1743–1752.

Hyuk Jin Kim is currently a Ph.D. candidate under the supervision of Prof. Ho Won Jang in the Department of Materials Science and Engineering at Seoul National University (SNU). He received his BS degree from the Materials Science and Engineering, Seoul National University, in 2022. His research focuses on chemoresistive liquid sensor based on 2D materials for electronic tongue.

Chung Won Lee is Postdoctoral Associate at University of Central Florida, Department of Materials Science and Engineering. He earned his Ph.D from the Department of Materials Science and Engineering, Seoul National University. His research focuses on electronic tongues based on 2D materials.

Sohyeon Park received her B.S. degree in chemical engineering and materials science from Ehwa Womens University in 2020. She is currently a Ph.D. candidate in materials science and engineering under the supervision of Prof. Ho Won Jang at Oxide Nanostructure & Nanoelectronics Laboratory, Seoul National University. Her research focuses on high-efficiency micro-LEDs and nanorod LEDs.

Sungkyun Choi is currently a Ph.D. candidate under the supervision of Prof. Ho Won Jang in the Department of Materials Science and Engineering at Seoul National University (SNU). He received his BS degree from the Materials Science and Engineering, Korea Advanced Institute of Science and Technology (KAIST), in 2018. His research interests include the synthesis and characterization of transition metal and single atom catalysts for energy conversion applications.

Sung Hyuk Park is currently a Ph.D. candidate under the supervision of Prof. Ho Won Jang in the Department of Materials Science and Engineering of Seoul National University (SNU). He received his BS degree in Materials Science and Engineering from Yonsei University, Seoul, Korea, in 2021. His current research focuses on the physics of hafnia-based ferroelectrics and the ferroelectric tunnel junctions of non-volatile memory devices.

Gi baek Nam is currently a Ph.D. candidate under the supervision of Prof. Ho Won Jang in the Department of Materials Science and Engineering of Seoul National University (SNU). He received his BS degree in Materials Science and Engineering from Korea University. His current research focuses on chemoresistive gas sensor based on 2D materials and metal oxides.

Jung-El Ryu is Postdoctoral Associate at the Department of Mechanical Engineering at Massachusetts Institute of Technology. He earned his Ph.D from the Department of Materials Science and Engineering, Seoul National University. His research focuses on high-efficiency micro-LEDs and micro-LED-based light-acti-vated gas sensors.

Tae Hoon Eom is Postdoctoral Associate at Research Institute of Advanced Materials, Department of Materials Science and Engineering, Seoul National University. He earned his Ph.D from the Department of Materials Science and Engineering, Seoul National University in February, 2022. His research focuses on visible light activated chemo-resistive gas sensor based on 2D materials and metal oxides.

Byungsoo Kim is currently a Ph.D. candidate under the supervision of Prof. Ho Won Jang in the Department of Materials Science and Engineering of Seoul National University (SNU). He received his BS degree in Materials Science and Engineering from Yonsei University, Seoul, Korea. His current research focuses on photodetectors using eptiaxy of Ga_2O_3 films.

Cheol-Joo Kim is an assistant professor in the Department of Chemical Engineering at POSTECH. He received his Ph.D. degree from POSTECH in 2011. His current research interests focus on the growth and structural engineering of two-dimensional materials for various nano-devices with advanced functionalities.

Soo Young Kim received his Ph.D. degree in Materials Science and Engineering from Pohang University of Science and Technology. After his postdoctoral period at Georgia Institute of Technology, he joined Chung-Ang University in 2009. Currently, he is a professor in the Department of Materials Science and Engineering at Korea University. He is interested in the modulation of the properties of 2D materials, such as graphene, graphene oxide, transition metal dichalcogenides, and halide perovskites, and their applications to various devices such as organic photovoltaics, perovskite solar cells, light emitting diodes, and gas sensors.

Ho Won Jang is a Full Professor in Department of Materials Science and Engineering at Seoul National University. He earned his Ph.D. from Department of Materials Science and Engineering at Pohang University of Science and Technology in 2004. He worked as a Research Associate at University of Wisconsin-Madison from 2006 to 2009. Before he joined Seoul National University in 2012, he had worked in Korea Institute of Science and Technology as a Senior Research Scientist. His research interests include the synthesis of oxides, 2D materials, and halide perovskites, and their applications in chemical sensors, nanoelectronics, solar water splitting cells, plasmonics, metal–insulator transition, and ferroelectricity.